BULLETIN OF THE POLISH ACADEMY OF SCIENCES
TECHNICAL SCIENCES, Vol. 71(6), 2023, Article number: e147918
DOI: 10.24425/bpasts.2023.147918

Kinovea analysis of high-speed video recording to determine kinematics of double pendulum in the long time scale

Jerzy WOJEWODA*

Division of Dynamics, Lodz University of Technology, Stefanowskiego 1/15, Lodz, 90-924, Poland

Abstract. Measurement of position and velocity of rotating objects relies on installation of additional devices, which can significantly change their dynamic properties. Non-contact methods appear not to have the above-mentioned drawback. To determine the angular kinematics, a video measurement technique stands as a non-contact alternative. The rotational motion can be recorded with a high-speed camera and then analyzed with free and open-source tracking software which allows one to detect and digitize positions of chosen markers and then to calculate angular positions of selected elements. Differentiation process determines rotary speed values. Analysis of long-term dynamical behavior by recording data visualized as *position maps* which possess half of the information usually stored in the well-known Poincaré maps is proposed.

Key words: angular position; rotary speed; video analysis; video tracking.

1. INTRODUCTION

Conventional methods for measuring the rotational speed of an object require installing a sensor device on it, such as a rotary encoder. However, attaching any additional elements can influence the physical properties of the object, such as the weight or moment of inertia. In contrast, non-contact measurement of the angular position using video tracking techniques is an alternative, which allows for maintaining the properties of the investigated object unchanged. The invented method of motion measuring was used to investigate the kinematics of the experimental double pendulum. The angular position is obtained by continuous tracking of characteristic points (markers) at consecutive video frames, digitizing the position data, and later in the differentiation process, velocities are calculated. This study proposes and develops a measurement technique based on available free software, which can be applied to study the behavior of complex dynamical systems on a large time scale.

The forced double pendulum system, which performs rotary motion, exhibits a richness of different behaviors, from simple periodic oscillations to almost periodic, an irregular combination of rotations and oscillations to rotations of both parts. Its dynamics have been investigated in many theoretical and experimental studies, e.g., [1, 2]. Such models can also produce chimeric behaviors, which have attracted attention recently. This has been proven experimentally in the rig of mechanical oscillators, which suggests that transient chimera-like states are observable in real-world networks [3]. These experiments have led to the discovery of long-transient state behavior [4]. To achieve progress in this matter, it is vital to establish methods that enable accurate, long-term measurements of kinematic quantities efficiently.

Techniques for measuring an object motion based on video tracking are adopted mostly in biomechanical applications to recognize the motion of limbs or gait [5]. They mostly consider low-speed recordings and analyzing of kinematic parameters of a single to few cycles of an object motion [6–8]. Paper [9] utilizes automatic object tracking by color for kinematic measurements processed by problem-oriented algorithms in MATLAB. It is prospective for kinetic and 2-D kinematic analysis of human dynamic standing balance. An example of the use of free software for motion analysis and measuring the relative knee angle of drop jump movement is shown in [10]. Interesting experimental data from a chaotic pendulum motion are presented in [11] where a method of using common hardware and software to synchronize angular readings of the pendulum with the phase of the driving system is presented. Poincaré sections can be displayed and analyzed.

Article [12] considers image processing methods for estimating the angles of the double pendulum. A significant number of transforms and computational procedures must achieve satisfactory results but on a short time scale. In [13] a new tracking algorithm for detecting the position of both links of a double pendulum which measures the angles of the links and computes uncertainties in the measured angles by following several trackers on each link is shown. Comparison of encoder and video-recognized data which were previously synchronized is presented. Well-related results are shown also on a short time scale. An example of using MATLAB in tracking the motion of a double pendulum is shown in [14], where the image analysis procedure of records from a high-speed camera is searched to find

*e-mail: jerzy.wojewoda@p.lodz.pl

Manuscript submitted 2023-02-01, revised 2023-09-23, initially accepted for publication 2023-10-08, published in December 2023.

© 2023 The Author(s). This is an open access article under the CC BY license (http://creativecommons.org/licenses/by/4.0/)

the centroid of the tracker in the image, but sometimes brute force and manual tracking is reported. Additionally, in [15] detection of the targets contrasting with the rest of the image in frames extracted from videos of a pendulum in a short time scale is shown. The application of MATHEMATICA in tracking the motion of a double pendulum using color markers is presented in [16]. A digital video camcorder was a source of analyzed frames extracted from the movies.

Long-term analysis of experimental systems is main subject of interest in investigating dynamical behavior. Article [17] shows long-term analysis based on MATLAB generated procedures but only a few points were collected. A mapping example shown in [18] presents practical application of long-time scale analysis of selected biomedical signals where mapping indicate healthy and disease states.

This paper is organized in the following way. Section 2 describes an experimental rig and hardware used in different stages of investigation, high-speed video data acquisition, marker tracking techniques, and the proposed method of computation the angles and velocities of both pendulums. Section 3 describes the validation of the collected data. Section 4 includes the main achieved results and finally, in Section 5 conclusions are drawn.

2. EXPERIMENTAL SETUP WITH A DOUBLE PENDULUM

A double-rotating pendulum reveals the richness of dynamic complexity of a simple physical system [1,2,19]. During earlier analysis, a set of 3 coupled double pendulums was used [3,4] in a synchronization investigation, but measurements of different motions were needed for experimental confirmation of numerical results. Therefore, for image-based measurements, a single pendulum set was considered, see Fig. 1(a). The motion of both pendulums could be continuously observed with a camera located directly at the mid-position of the supporting axis height (point O_1 in Fig. 1(b)) and perpendicular to its plane of motion.

The set was fixed to a LDS V780 shaker head. Both pendulum bodies were manufactured as aluminum beams and their weights were adjusted to the required values using additional brass masses to avoid interaction with the electromagnetic force generated by the shaker. The parameter values were established earlier in a series of numerical simulations [3,4] to achieve all types of desired behavior. All bearings are made of low-friction plastic materials. Such properties minimize any possible influences from the electromagnetic field created in the shaker.

High-speed Phantom v711 camera was used in experiments. It can take a maximum of 7530 fps at full 1280×800 px monochrome resolution. Two types of contrasting markers were used – either made with UV paint or printed black-on-white ones that had forms of different geometric shapes such as a point, ring, or cross and were placed at characteristic points of both pendulums while the background was kept dark. Fluorescent and LED marker setups are shown in Figs. 1(c) and 1(e), and some non-uniformity of the background can be noticed. The light sources were either UV or LED lamps. The 3 predefined markers stated a measurement base and did not require any additional image processing at the recognition stage which was performed by free and open-source software.

2.1. Measurement technique

Experimental data obtained from video recording were stored as long sequences of consecutive images that later were the subject of analysis. A smooth picture of time histories required a high sampling rate, while for mapping purposes a single image per excitation cycle was sufficient. Sequences of digital images allow one to track marker positions and digitize them into $x-y$ coordinates measured in pixels. Important advantage of applying tracking software over probes and sensors is the possibility for the study of 2-D motion, such as revolving elements or projectiles without any wiring or attaching sensors. Also more than one object can be analyzed in a single video recording. Use of the existing and effective software does not need to build custom programs, which usually need many image processing operations before tracking itself, like [12]. There exist known limitations and disadvantages of video analysis as limited video record resolution, which depends on the camera capabilities. The larger the picture size, the better the results in determining the position of the tracked markers. Recording speed determines the capability of observation of quick events and is strictly determined by the hardware in the camera. Memory capacity – its buffer size determines the amount of data stored in the camera memory, which is simply the length of the available time history.

2.2. Tracking software

Most of the existing free tracking software is intended for biomechanical tasks and industrial applications, which re-

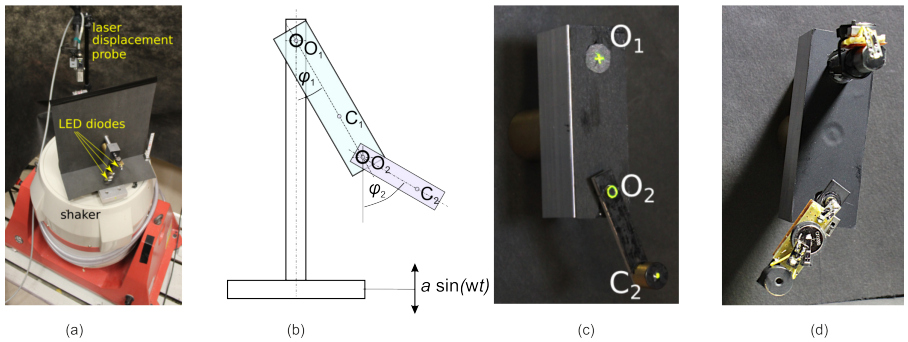

Fig. 1. Experimental rig: (a) general view, (b) physical model, (c) fluorescent markers and (d) LED arrangement

quire frequent manual user interaction. For long-term analysis extending to thousands of motion periods, a program in which user input is restricted to the declaration of points of interest and export of the analyzed data is needed. Several available programs with tracking capabilities have been tested to effectively analyze such image sequences. Typical examples include commercial and costly image recognition and analysis software such as VICON, QUALISYS, TEMA, SIMI, POLHEMUS. They are sometimes connected with specific hardware only, which increases costs, so it is not easily available even for testing purposes. Therefore the preferable solution was free and open source software such as MOKKA, TRACKER or PHYSMO[1] were tried. They require manual interaction from the user to prevent losing the tracked marker. In the investigated case, an automated procedure was required for many video file analyses, and KINOVEA appeared to be the most effective[2], simple and cost-free solution.

In all analyzed cases of image the tracking process did not require any pre- or post-processing of the recorded movies. Kinovea automatic tracking works by computing the cross-correlation coefficient between a candidate window and the feature window of the previous image. For each possible position in the search window, a score is calculated, and the best score is the match (unless it is under a specific threshold in which case we assume the target was lost). Therefore, it is a measure of how much the candidate looks like the original. Based on the theory – the preferred are circular markers, having a color and brightness contrast with a background that is not present in the rest of the search window. It is not invariant to rotation, so if rotating the marker changes its look, it will be harder to match. It will look at the immediate surroundings, so having a target that does not resemble any other part of its vicinity is better to avoid mismatches. Many of performed experiments required analysis of a time span as large as possible for estimating the character of the object motion that includes forms of both periodic and irregular ones. When long-term behavior is to be analyzed, the most useful are Poincaré maps, which can be understood as the intersection of a periodic orbit in the state space of a continuous dynamical system with a certain lower-dimensional subspace like position-velocity coordinates checked after every period of the excitation force. From time histories that last 5–30 seconds at rather low-frequency shaker excitation f (appr. 5 Hz), there is a possibility of extracting up to approximately 25–150 consecutive readings only.

The KINOVEA search areas are the smaller rectangles shown in Fig. 2. The tricky aspect is choosing their sizes (larger rectangles) that do not overlap too much in any frame. The traces shown here represent the last N frames ($1 \leq N \leq 200$). Note the different lengths of the analyzed paths strictly visually reflecting velocities in the displayed time span.

[1] www.vicon.com, www.qualisys.com, www.imagesystems.se/tema, www.simi.com, polhemus.com/motion-tracking/all-trackers, biomechanical-toolkit.github.io/mokka, physlets.org/tracker, physmo.sourceforge.net

[2] www.kinovea.org/ – declares: *Kinovea is a video player for sports analysis. It provides a set of tools to capture, slow down, study, compare, annotate and measure technical performances. Kinovea is free and open source.*

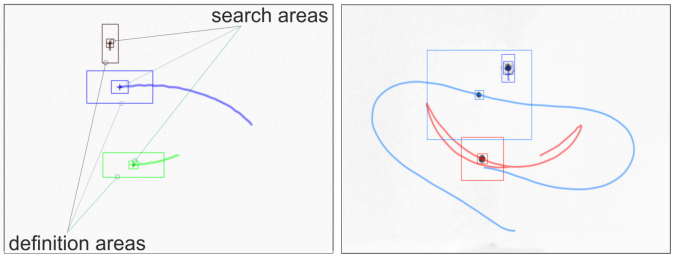

Fig. 2. Examples of frames used in the KINOVEA for the analysis of irregular motion, search and definition are shown

2.3. Image recognition errors

The use of tracking software involves some obvious errors because the base of the recognition is always a recorded bitmap, which is a rectangular matrix of pixels. Therefore, at least two factors are to be included in error analysis – the absolute size of the marker detected and its relative dimensions with respect to the size of the analyzed bitmap.

A typical layout of the recognition area is shown in Fig. 3. Enlarged parts show the source of errors as a position of the tracked marker may appear anywhere inside the red circles; therefore, the detection process can return any value between α_1 and α_2 angles. An arbitrary position of 3 markers O_1, O_2, and C_2 are shown together with a more detailed view of the small pendulum and magnifications of its markers. All of them are larger than a single pixel in the recorded bitmap, and their positions are determined by two sets of coordinates $(x_0, y_0) - (x_1, y_1)$ for the large pendulum and $(x_1, y_1) - (x_2, y_2)$ for the small pendulum. $\Delta x = x_2 - x_1$ and $\Delta y = y_2 - y_1$ allow the determination of the function of the actual inclination value.

$$\alpha = f(x_1, x_2, y_1, y_2) = \arctan \frac{y_2 - y_1}{x_2 - x_1} = \arctan \frac{\Delta y}{\Delta x}. \quad (1)$$

Recorded diameters of both markers are equal to K_i $(i = 1, 2)$ pixels. The horizontal and vertical sizes of the bitmap are N by M pixels. The distances between the markers (pendulum lengths) are $L_1 = |O_2 - O_1|$ and $L_2 = |C_2 - O_2|$, both in pixels. Tracking results can appear inside any pixel within both marker circles, so in any position, we can obtain an error $\Delta\alpha = \alpha_2 - \alpha_1$. Such a process does not lead to cumulative errors, as any next frame has similar properties as the earlier one and no influence

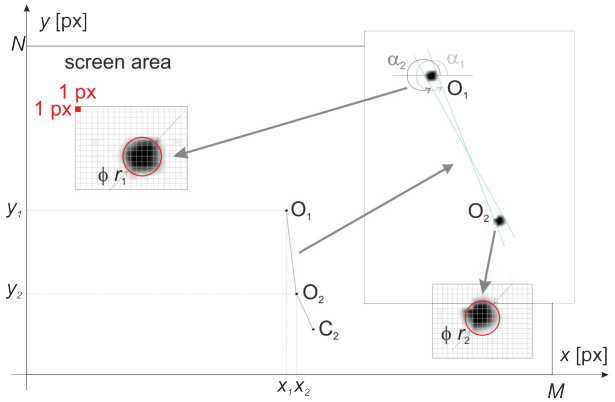

Fig. 3. A frame from a recorded video used for tracking

is transferred from the previous recognition stage. The derivatives are:

$$\begin{aligned}
\frac{\partial f}{\partial x_1} &= \frac{y_2-y_1}{(y_2-y_1)^2+(x_2-x_1)^2} = \frac{\Delta y}{L^2} = \frac{\sin\alpha}{L},\\
\frac{\partial f}{\partial x_2} &= -\frac{y_2-y_1}{(y_2-y_1)^2+(x_2-x_1)^2} = -\frac{\Delta y}{L^2} = -\frac{\sin\alpha}{L},\\
\frac{\partial f}{\partial y_1} &= -\frac{x_2-x_1}{(y_2-y_1)^2+(x_2-x_1)^2} = -\frac{\Delta x}{L^2} = -\frac{\cos\alpha}{L},\\
\frac{\partial f}{\partial y_2} &= \frac{x_2-x_1}{(y_2-y_1)^2+(x_2-x_1)^2} = \frac{\Delta x}{L^2} = \frac{\cos\alpha}{L}.
\end{aligned} \tag{2}$$

The total differential $d\alpha$ of the function f is as follows:

$$d\alpha = \frac{\partial f}{\partial x_1}dx_1 + \frac{\partial f}{\partial x_2}dx_2 + \frac{\partial f}{\partial y_1}dy_1 + \frac{\partial f}{\partial y_2}dy_2\,. \tag{3}$$

We can estimate the upper limit of recognition error (depending on α) as:

$$\Delta\alpha = \left|\frac{\partial f}{\partial x_1}r_1\right| + \left|\frac{\partial f}{\partial x_2}r_2\right| + \left|\frac{\partial f}{\partial y_1}r_1\right| + \left|\frac{\partial f}{\partial y_2}r_2\right|, \tag{4}$$

whose magnitude is bound from above:

$$\begin{aligned}
\Delta\alpha &= \left|\frac{\sin\alpha}{L}r_1\right| + \left|\frac{-\sin\alpha}{L}r_2\right| + \left|\frac{\cos\alpha}{L}r_1\right| + \left|\frac{-\cos\alpha}{L}r_2\right|\\
&= \frac{r_1}{L}(|\sin\alpha|+|\cos\alpha|) + \frac{r_2}{L}(|\sin\alpha|+|\cos\alpha|)\\
&= \frac{r_1+r_2}{L}(|\sin\alpha|+|\cos\alpha|) \le \frac{r_1+r_2}{L}\sqrt{2}\,.
\end{aligned} \tag{5}$$

This simply means that the maximum error is smaller than the above-calculated value. If $r_1 = r_2 = r$, the upper limit of the estimation error is as follows:

$$\Delta\alpha_{\max} = 2\sqrt{2}\frac{r}{L}\,. \tag{6}$$

In summary,

$$\alpha \in [f(x_1,x_2,y_1,y_2) - \Delta\alpha_{\max}, f(x_1,x_2,y_1,y_2) + \Delta\alpha_{\max}], \tag{7}$$

where: $\Delta\alpha_{\max} = \sqrt{2}\frac{r_1+r_2}{L}$, when $r_1 \neq r_2$ or $\Delta\alpha_{\max} = \frac{2r}{L}\sqrt{2}$ when $r_1 = r_2 = r$.

For a typical recognition process based on an image frame of 800×600 px it has been found $r_1 = 4$ px, and $r_2 = 3.5$ px, so $r = 4$ was taken. For $L = 207$ pixels, the maximum estimation error value was calculated as 3.124 deg. The upper error bound for the angle of the secondary pendulum is expected to be inversely proportional to its length, see equation (6). The noise level in the measured signals was established by analysis of test results performed in the arrangement the test rig where the double pendulum remains at rest. Records sampled at 450 fps for 36.9 s were recorded and statistics of the recognized angle value were calculated. The expected values of the measured angles were zero but showed a dispersion of values of ± 0.002 rad, see the example in Fig. 4. This value was related to the $[-\pi, +\pi]$ range resulting in a relative measurement error of 0.064%. The value of counts stands for number of detected results in the appropriate bin within all analyzed data.

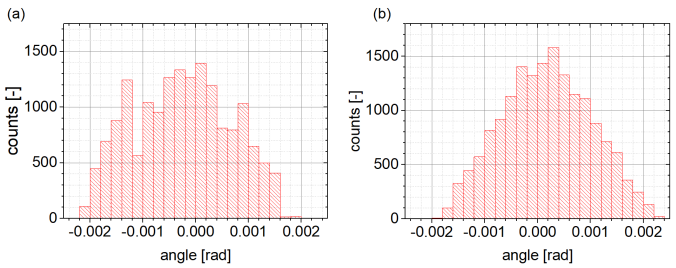

Fig. 4. Statistical analysis of noise estimation of recognized angles

An example of the position digitized signal is shown in Fig. 5(a). It presents the recorded time history of the large pendulum excited axis position. Flat segments (limitations of pixel-size recognition) appear in the graph when changes of the pendulum angle are too small to be detected. There exists a possibility of smoothing angular data at this stage, but to avoid that, smoothing (or filtering) was done after differentiating, i.e., applied to angular velocity data. The recognition errors continue their effects in the next stage of the evaluation of angular velocity, which is obtained by the differentiation of angle values.

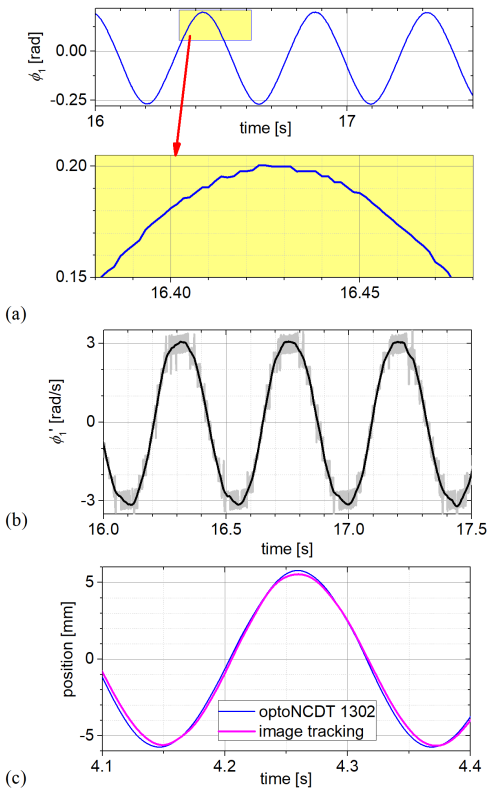

Fig. 5. Experimental time histories: (a) details of recognition accuracy, (b) calculated velocity: raw data (gray) and 20 pts smoothing (black) and (c) comparison of recognized data and external measurements

This was performed on digitized results outside the recognition program using the Savitzky-Golay procedure 2nd order polynomial smoothing, which was adequate to obtain a smooth derivation of the angular velocity values, see Fig. 5(b). The results of displacement measurements obtained from the external optoNCDT 1302 laser sensor (blue) compared with those from image recognition and tracking results (magenta) are shown in Fig. 5(c). Laser sensor delivered results which were assumed to be real while tracing delivered values smaller by approximately 3.5%, which can be caused by the limited resolution of the analyzed images (1280 × 800 px).

3. QUALITY OF THE RESULTS ON A SHORT TIME SCALE

A numerical model with equations and data parameters can be found in [3] together in relation to the experimental one. The examples below show the efficiency of the image recognition method used in experiments. Each case was later performed numerically for equivalent experimental parameters. Figure 6 shows a comparison between the simulation and measurement results for irregular and rotational motion. The quality of the results appears very satisfying in all cases. Quantitative differences may be result of the small inaccuracy of system parameter estimation.

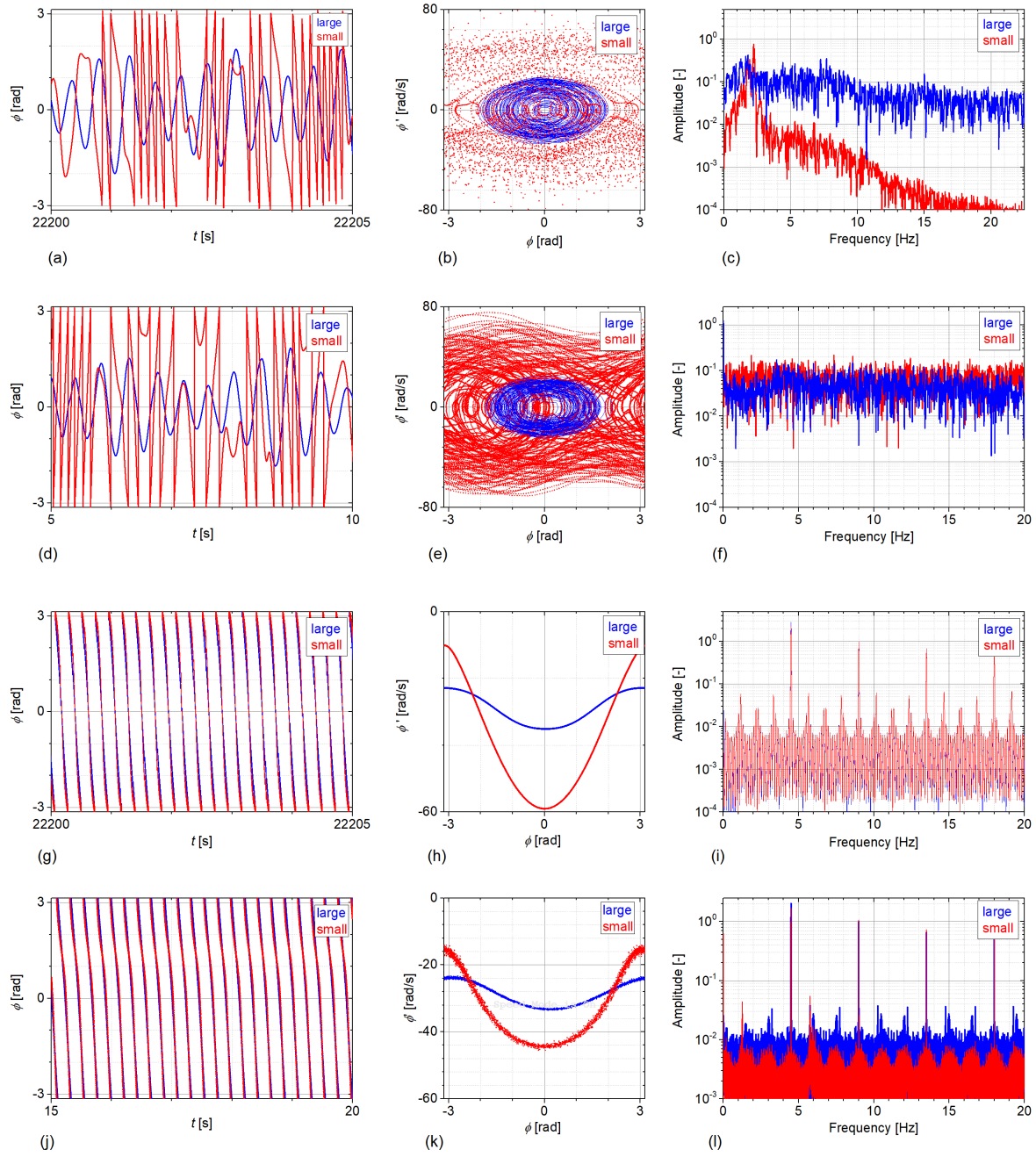

Fig. 6. Time histories (left), phase plane trajectories (middle), and amplitude spectra (right). Irregular motion at $A = 4.7$ mm, $f = 4.5$ Hz. Numerical results: (a)–(c); experimental: (d)–(f). Rotations at $A = 7.4$ mm, numerical: (g)–(i), and experimental: (j)–(l)

Another measure of quality is FFT frequency analysis of the experimental data recorded and digitized, and those from numerical simulations shown in Fig. 6. Comparison of these results also presents satisfactory agreement. All experimental data were sampled at 45 Hz (10 times per excitation cycle) show similar-dominating frequencies. Amplitudes are also analogous in all cases of the noted motion, from small oscillations with 1 cycle per two excitation cycles of almost periodic type through irregular with noisy character (half of the excitation frequency dominates in both cases). Usually, there is a combination of oscillations of the large pendulum and mixed oscillations/rotations of the small pendulum to full rotations of both elements. In a rotating motion the dominating frequency equals to the excitation one. In the case of numerical simulations based on the modeled system equation, see [3], its parameters were chosen to reflect the respective experimental runs, and the results of frequency analysis are similar and have less noise detected.

3.1. Determination of experimental time histories

The digitization process in the tracking software requires some manual adjustment of search patterns and their areas depending on the distances between markers in consecutive frames. Obviously, as sampling increases, increments of positions between the consecutive points diminish. Therefore, the process is much easier with high sampling rates but tends to result in more noisy data. The search areas in Kinovea for high-speed data were relatively small, and consecutive points appeared at a close distance. Such an attempt is suitable for rotations or small oscillations of both pendulums. In the investigated rotary motion sampling rate being about 100 times higher than excitation frequency delivers smooth signals and does not require any processing. Small pendulum usually rotates faster and sampling rate should be accordingly higher.

As presented in Fig. 7, smoothing of the angle signal derivative delivers satisfying quality when amount of locally considered in the Savitzky-Golay method stays below 100 points. It performs a polynomial regression to the data points in the moving window. Then output data point is computed as the value of the polynomial at the local position. Increase in the number of such points leads to some distortion of the rotation speed values – blue trace. All smoothing tends to small diminishing of the speed amplitudes. FFT low-pass filtering with limit frequency of a value of 5 times more than the excitation one seems to be the most effective method.

In adequately sampled recognized signals (100–200 samples per second) derivation of raw signal with 25-points Savitzky-Golay smoothing delivers similar results as derivation of low-pass filtered raw signal with no smoothing at this stage. As presented in Fig. 8 low-pass filtering at cut-off frequency 22.5 Hz and Savitzky-Golay smoothing at both stages of calculation deliver similar results in calculating the rotation speed.

3.2. Calculation of experimental rotational velocities

All further calculations – differentiation, smoothing, filtering were performed to recognized data sets with free data analysis software like SciDavis or Qtiplot. Rotational velocities $\dot{\phi}_i(t)$ were calculated by the differentiation of the t_i, ϕ_i data by the

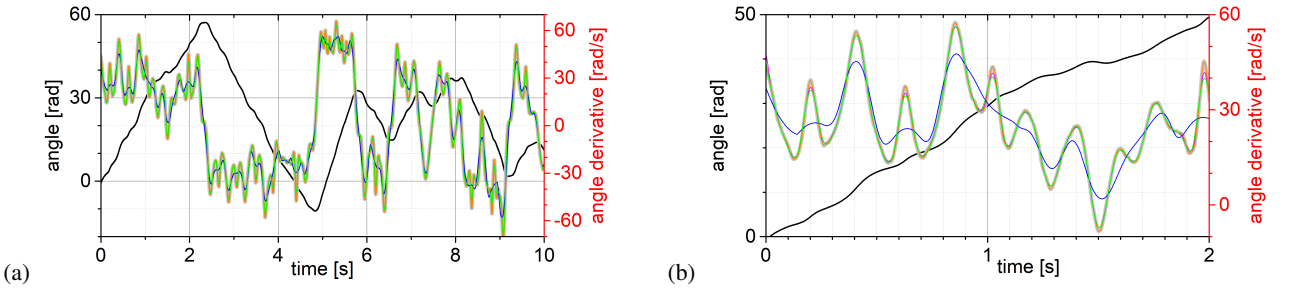

Fig. 7. Small pendulum in arbitrary motion – recognized angle (black) and its derivative signals (rotation speed, colored traces) filtered/smoothed in different ways at sampling rate of 900 fps – left, and its magnified part – right

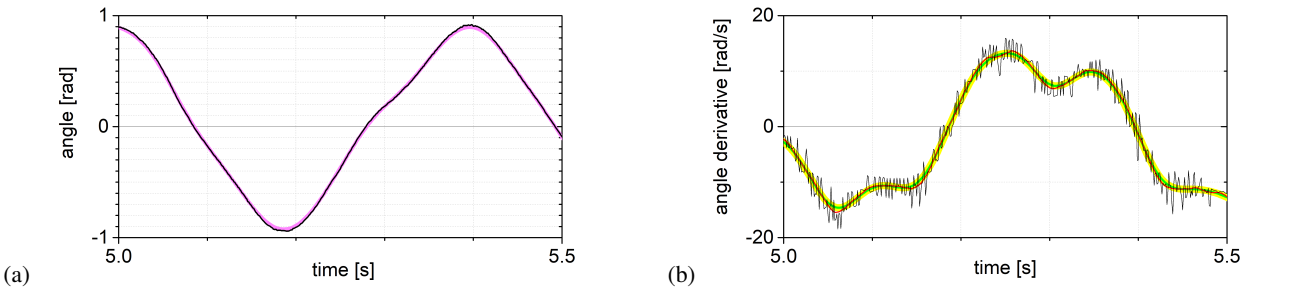

Fig. 8. Large pendulum: (a) recognized angle (black) and its low-pass filtered signal at cut-off frequency 22.5 Hz (magenta), and (b) comparison of derivative procedures: no processing of angle data (black), 22.5 Hz low-pass derivative of raw angle data (yellow), raw derivative of 22.5 Hz low-pass filtered angle (green), 25 points Savitzky-Golay smoothed derivative of Savitzky-Golay 25 pts smoothed angle (pink)

transform of the centered difference formula and calculates the derivative at a point by taking the average of the slopes between the point and its two closest neighbors. As the original angle data result from the digitization of limited-resolution video files and significant oversampling at 6000 fps and for testing purposes were not subject to any smoothing, differentiation leads to noisy derivative graphs. Therefore, some processing has been applied to the velocity signals in two ways, either by calculating the running average of the derivative data, Fig. 9(a) or by applying the FFT low pass filter with a cutoff frequency being 10 times higher than the excitation one, i.e., 45 Hz, Fig. 9(c). Both processes deliver similar results in terms of quality and quantity. Differentiation of smoothed ϕ_i signals required up to 250 pts to achieve similar results, Fig. 9(b). Low-pass filtering at cut-off frequency 5–10 times higher than excitation frequency was found as most efficient. As obtaining accelerations needs another differentiation stage and yet more processing, an example is shown in Fig. 10(b).

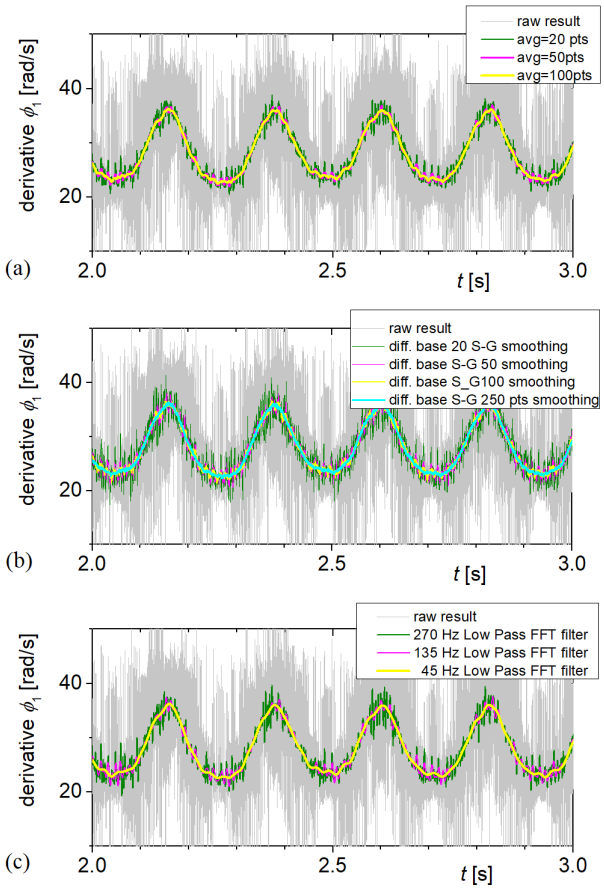

Fig. 9. Different approaches to determine experimental rotation speed: (a) simple averaging of the angle derivative at 20, 50, 100 pts, (b) Savitzky-Golay smoothing derivatives of smoothed angles ϕ_1 averaged at 20, 50, 100, 250 pts, and (c) FFT low-pass filtering of the angle derivative with cut-off frequencies 270, 135, 45 Hz

There exists possibility of calculating even rotary acceleration signals with reasonably smooth traces obtained after low-pass filtering with cut-off frequency of 22.5 Hz, see Fig. 10(b).

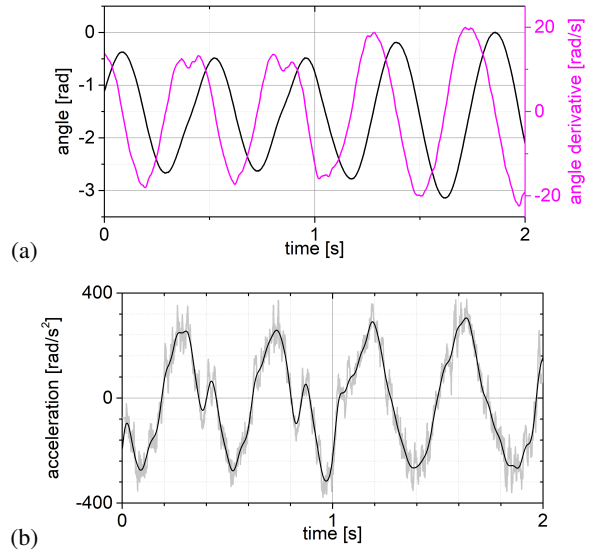

Fig. 10. Large pendulum – (a) recognized angle (black) and its derivative (rotation speed, magenta) without any processing at sampling rate of 450 fps, and (b) calculated acceleration signal: gray and low-pass filtered at 22.5 Hz: black

4. LONG-TIME SCALE APPLICATION – DETERMINATION OF THE POSITION MAPS

In dynamical systems, the first recurrence map or Poincaré map is the intersection of an orbit in the state space of a continuous dynamical system with a certain lower-dimensional subspace, called the Poincaré section, transversal to the flow of the system [20]. Typical creation of a Poincaré map, needs choosing a specific phase space (e.g., position and velocity) and plot the points where the pendulum crosses a particular surface or plane in that phase space. For a double pendulum, this could involve plotting the angle and angular velocity of both masses after every period of the excitation force. By repeating this process for multiple cycles of the pendulum motion, a Poincaré map is created that shows the long-term behavior of the system. It can provide insights into the stability, periodicity, and chaotic behavior of the double pendulum.

As velocity data are difficult to calculate at a low sampling rate in mapping tasks, the digitization process can deliver another type of mapping – *position map* recorded in a way similar to collecting data for Poincaré maps – here samples are taken after every period of excitation. For obvious reasons (as the next sample occurs in time which does not allow for calculating actual velocity at this point) it can store only the position value. Therefore, the map contains half of the information that is normally stored in Poincaré maps which in the case of a single pendulum are points in $\phi - \phi'$ state space, a dimension of 4 is reduced to 2.

During the experiments, two techniques for collecting simplified maps were developed – by use of a DSLR camera working in triggered mode and quick camera movie recordings. Long-term observation forces a less frequent sampling rate, which is triggered at the same moment in every cycle of the forcing. The method facilitates the detection of ϕ values only and there is no chance to store two (or a few more) consec-

utive frames in the vicinity of the trigger occurrence. This is how the classical camera works – only a single exposure can be triggered in the assumed period. For quick camera the size of the memory buffer is the limit which prevents collecting data in a way which can allow for calculating velocity in a mapping point.

4.1. Use of the DLSR still camera

The first method was the use of a standard digital camera, which was triggered by an event-based, custom-made external electronic device releasing the Canon 5D DSLR camera mechanical shutter for every period of excitation force. The triggering device was connected to a Hameg HMF2525 arbitrary function generator as an input source also for the shaker and outputs as an external trigger to the camera. Then, all stored photographs were collected into a movie using FFMPEG-free software. The video was then a subject of tracking analysis, which delivered digitized data on the positions of all markers. The technique is useful up to a maximum speed of continuously shooting speed of the particular camera (6 fps, i.e., 6 Hz sampling rate). The main limitations are internal memory buffer size and transfer speed to external storage. We do not consider any movie modes in DSLR, as external hardware triggering is used as a control of the camera. In the experiments, the camera speed of 4.5 fps was sufficient for a continuous record of at least 12 min of the rig run, which corresponds to a series of more than 3200 photographs (periodical views). Figure 11 shows a unique example of the *position map* for irregular motion. It was made as a single image composed of the overlay of a long series of separate digital camera photographs in UV light.

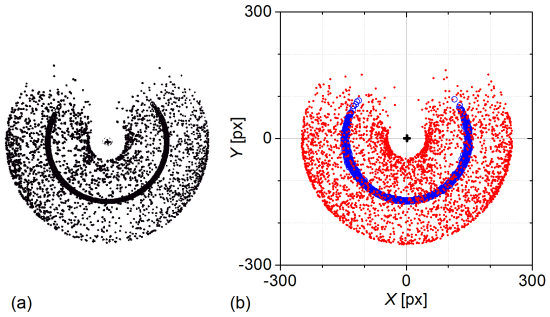

Fig. 11. Position maps for the irregular motions composed of 2711 still images by DSLR, excitation parameters $A = 4.10$ mm, $f = 4.50$ Hz: (a) negative view and (b) another run after digitization, 3069 recognized points

4.2. Use of the Phantom v711 high-speed camera

The other method used in another series of experiments was the usage of a high-speed camera, which is designed to collect images only in the movie mode. The minimum recording speed of approximately 22 fps was too high to be equal to the excitation frequency of 4.5 Hz, therefore a multiple of the frame rate had to be chosen, the factor of 10 giving 45 fps was applied. The camera memory buffer can hold about 32000 frames of the record, covering up to 3200 periods of excitation in over 11 min run. Then, the FFMPEG program extracted every 10^{th} frame and removed all others. Another pass-through FFMPEG produced the composition of a new video containing only the chosen frames. KINOVEA then analyzed the created video file.

4.3. Comparison with Poincaré maps

As a measure of information value delivered by the map as shown in Fig. 11, a comparison with numerically calculated Poincaré maps is shown in Fig. 12.

Projections to the lower dimension of ϕ of the experimentally recorded results are compared to numerical simulations collected for both pendulum rotation angles. The irregular dynamics are reflected in both, the experimental and simulation data sets. Similar results can be shown for other types of behavior, such as periodic oscillations or rotations. A full view of the Poincaré map from numerical simulations is shown in Fig. 12(e). Unfortunately, no experimental comparison is available, as the method does not allow for obtaining rotation velocity together with position values due to the lack of neighboring point values for calculations. Therefore, a position map such as that shown in Fig. 11 can be used. In both of them, the points corresponding to the large pendulum are dispersed along the angle axis, as they simply represent a projection to this axis. Example of experimentally collected Poincaré map is shown in Fig. 12(b) as plot of the points over complete trajectories of the motion in the irregular case. Data collected at 900 fps delivered 158 map points, see Fig. 12(b). When the sampling rate increases the recognized data were more detailed at a cost of the record length with limit of the memory buffer size. Figure 13 shows examples of *position maps* collected in this way for quasiperiodic, irregular, and oscillating types of motion.

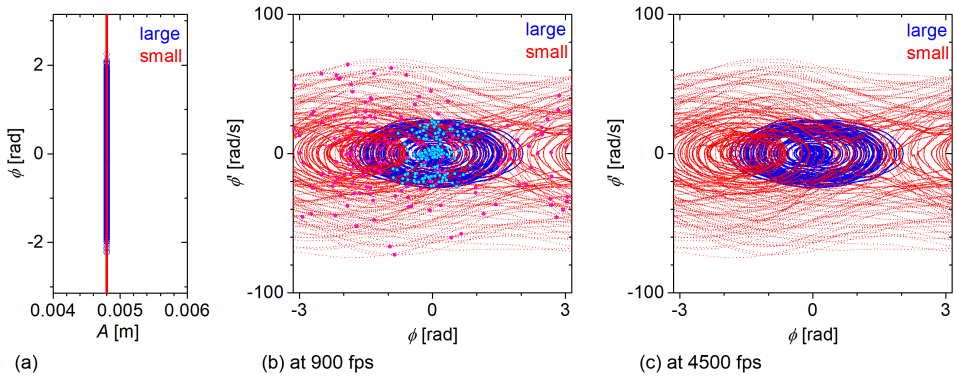

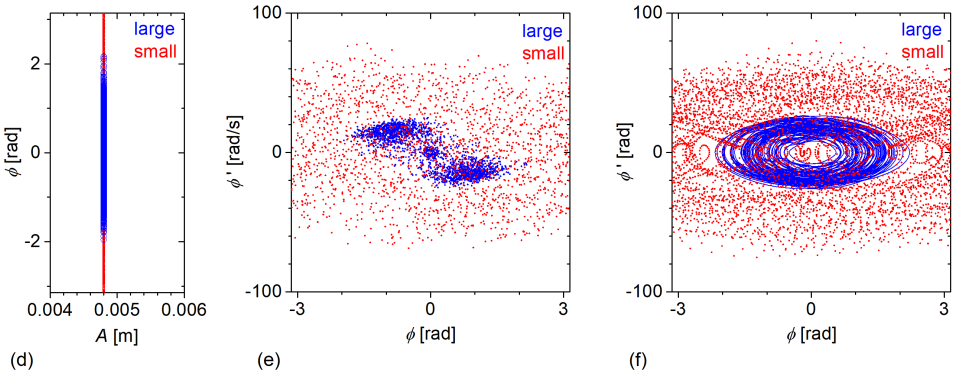

Fig. 12. Comparisons of experimental (top) and numerical (bottom row): projections of Poincaré maps for irregular motion collected at over 2000 excitation cycles at shaker parameters $A = 4.8$ mm and $f = 4.5$ Hz – (a) and (d); Poincaré maps – (b) and (e); trajectories – (c) and (f). Note, that the lengths of the records were not equal

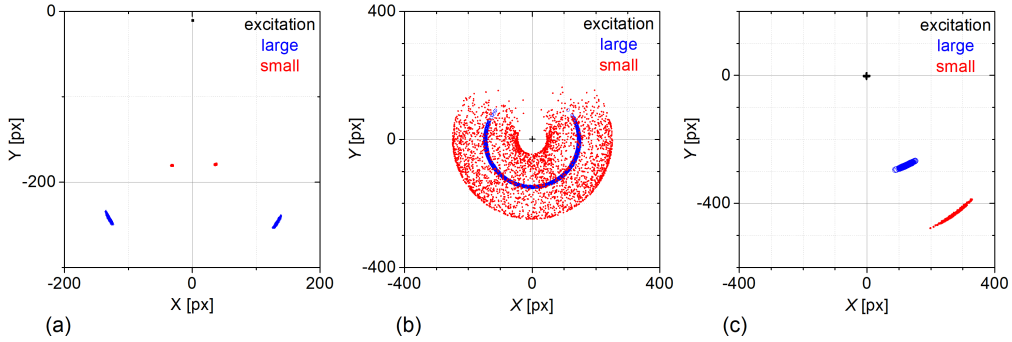

Fig. 13. Digitized *position maps* collected experimentally at $f = 4.5$ Hz: (a) rotations, DSLR 2300 frames (1920×1080 px) at $A = 7.2$ mm; (b) irregular behavior; Phantom v711, 3069 frames, $A = 4.9$ mm and (c) small oscillations; Phantom v711, 1650 frames, $A = 3.8$ mm

5. DISCUSSION AND SUMMARY

The proposed method for measuring the rotation angle based on tracking the image data stored in video file is presented. It is relatively simple and effective, and uses freely available software although it requires some efforts in the preparation of the rig, as markers, background, lightning. Performing long term measurements requires a choice of recording parameters for high-speed digital camera, or applying an external system to trigger a DSLR camera shutter. Preparation of video files composed of single photographs, or decomposing a high-speed camera record into separate images and choosing particular frames, which are then composed into a new video file for tracking and determination of the *position maps*. Occasional, manual adjustments in the tracking search areas must be applied in difficult cases with quickly moving markers: calculating angle values from the digitized data then calculation of the derivative(s) of the angle data with smoothing or low-pass filtering.

The results in the form of angle and rotational velocity time histories agree qualitatively and quantitatively with the simulation data. Examples of such comparisons are presented. Increasing the resolution of the source video results in more exact angle values. It is important to ensure that trajectories fill most of the frame areas. In cases where the measurement goal is to reflect detailed time history at a higher sampling rate, it leads to an easier process and improves its accuracy. Oversampling leads to noisy results and requires post-processing in form of Savitzky-Golay smoothing ot better low-pass filtering with cut-off frequency being 5 times higher than excitation one.

A mapping system called a *position map* was proposed. It can be interpreted as a projection of a 4-dimensional Poincaré map to a 2-dimensional space. It facilitates visual evaluation of the system behavior. Such *position maps* present a similar layout of detected values as can be found in standard Poincaré maps.

There is an important advantage of measurements performed with the help of this method which is not introducing any sensors, only the placement of markers, which do not change the dynamic properties of the system, and neither wires nor external measuring devices are present. Obtained accuracy may depend on the tracker applied but can be reliable for measurement of angles and satisfying for calculated velocity and acceleration values.

ACKNOWLEDGEMENTS

The author thanks Bogdan Jagiełło and Wiesław Prus in creating arrangements, equipment and for technical assistance during the experiments.

REFERENCES

[1] T. Shinbrot, C. Grebogi, J. Wisdom, and J.A. Yorke, "Chaos in a double pendulum," *Am. J. Phys.*, vol. 60, no. 6, pp. 491–499, 1992.

[2] R.B. Levien and S.M. Tan, "Double pendulum: An experiment in chaos," *Am. J. Phys.*, vol. 61, p. 1038–1044, 1993.

[3] D. Dudkowski, J. Wojewoda, K. Czolczynski, and T. Kapitaniak, "Transient chimera–like states for forced oscillators," *Chaos*, p. 011102, 2020.

[4] D. Dudkowski, J. Wojewoda, K. Czolczynski, and T. Kapitaniak, "Is it really chaos? the complexity of transient dynamics of double pendula," *Nonlinear Dyn.*, vol. 102, pp. 759–770, 2020.

[5] J. Poonyawatpornkul and P. Wattanakasiwich, "High-speed video analysis of damped harmonic motion," *Phys. Educ.*, vol. 48, no. 6, p. 782, 2013.

[6] "Step by step and frame by frame – workflow for efficient motion tracking of high-speed movements in animals," *Zoology*, vol. 141, p. 125800, 2020.

[7] M.M. Baclig, N. Ergezinger, Q. Mei, M. Gül, S. Adeeb, and L. Westover, "A deep learning and computer vision based multiplayer tracker for squash," *Appl. Sci.*, vol. 10, no. 24, p. 8793, 2020.

[8] N. Feng and P. Gao, "The accurate repair of image contour of human motion tracking based on improved snake model," *Complexity*, 2021.

[9] K. Kirilova and P. Gatev, "A complex semi-automatic method for kinetic and two-dimensional kinematic motion analysis for posture and movement investigation," *Int. J. Bioautomotion*, vol. 22, no. 1, 2010.

[10] N. Adnan, M.A. Patar, H. Lee, S.-I. Yamamoto, L. Young, and J. Mahmud, "Biomechanical analysis using kinovea for sports application," in *IOP Conference Series: Materials Science and Engng*, 2018, pp. 1–9.

[11] R. DeSerio, "Chaotic pendulum: The complete attractor," *Am. J. Phys.*, vol. 71, pp. 250–257, 2003.

[12] M. Haris, J. Memon, and M. Farhan, "Image processing techniques for fast and accurate estimation of pose of a double pendulum," in *4th International Conference on Computer Graphics, Visualization, Computer Vision and Image Processing. Zagreb, Croatia, 2020*, May 2020, pp. 232–236.

[13] A. Myers, J.R. Tempelman, D. Petrushenko, and F.A. Khasawneh, "Low-cost double pendulum for high-quality data collection with open-source video tracking and analysis," *HardwareX*, vol. 8, pp. 1–23, 2020.

[14] G. Lee, "The simulation and analysis of a single and double inverted pendulum with a vertically-driven pivot," 2011, School of Physics, Georgia Tech.

[15] P. Devaux, V. Piau, O. Vignaud, G. Grosse, R. Olarte, and A. Nuttin, "Cross-camera tracking and frequency analysis of a cheap slinky wilberforce pendulum," *Emergent Scientist*, vol. 3, no. 1, 2019.

[16] C. Kulp, D. Schlingmann, P. Ramsey, J. Hoskins, and K. Roberts, "Tracking the motion of a double pendulum using mathematica," *J. Plan. Educ. Res.*, vol. 12, no. 2, pp. 99–109, 2007.

[17] J.Z. Blumoff, "Exploration of the double pendulum," 2010, Georgia Institute of Technology, Atlanta, Georgia.

[18] A.K. Golinska, "Poincaré plots in analysis of selected biomedical signals," *Stud. Log. Gramm. Rhetor.*, vol. 48, no. 35, 2013.

[19] Y. Liang and B. Feeny, "Parametric identification of a chaotic base-excited double pendulum experiment," *Nonlinear Dyn.*, vol. 52, p. 181–197, 2007.

[20] T.S. Parker and L.O. Chua, *Practical Numerical Algorithms for Chaotic Systems*. New York, Berlin, Heidelberg: Springer, 1989.